

Typical Applications of MARY Spectroscopy: Radical Ions of Substituted Benzenes

E. V. Kalneus^{1,2}, D. V. Stass^{1,2}, and Yu. N. Molin¹

¹ Institute of Chemical Kinetics and Combustion, Russian Academy of Sciences, Novosibirsk, Russian Federation

² Novosibirsk State University, Novosibirsk, Russian Federation

Received October 12, 2004

Abstract. The paper describes the underlying principles and discusses the most important advantages and limitations of the experimental technique of magnetically affected reaction yield spectroscopy as developed in the authors' laboratory and guides the reader step by step through a typical experimental sequence using as example the problem of short-lived radical cations of a series of methyl-substituted benzenes in X-irradiated nonpolar solutions. For two of the eight target substances – benzene itself and mesitylene – the paper reports the first unequivocal observation of their radical cations in liquid alkane solution at room temperature and provides a lower estimate of about 10 ns for their relaxation times in low magnetic field.

1 Introduction

Magnetically affected reaction yield (MARY), or level-crossing, spectroscopy is a relatively recent addition to the family of spin-chemistry techniques that are widely used in modern chemistry and biology to study processes involving formation and elimination of short-lived paramagnetic intermediates – neutral radicals and radical ions, metastable triplet states, etc. – as one of their critical stages [1, 2]. The presence of uncompensated electron spin allows to control these processes by applying external magnetic fields, thus altering the course of the reaction. Furthermore, the spins are usually produced as correlated pairs, with correlation persisting long enough for coherent effects in the spin system to play their role. Often this coherence can be used to advantage to create new methods for probing spin systems under conditions that are normally unacceptable for the more conventional magnetoresonance techniques. Manifestations of spin coherence in pulsed nuclear magnetic resonance (NMR) and electron spin resonance (ESR) are well known and form the basis for their modern methodology. Less widely used, but well understood and documented are coherent phenomena

in continuous-wave (CW) ESR [3, 4]. However in MARY spectroscopy, coherent effects work alone to provide spectral and kinetic information without external microwave or radio-frequency pumping, and in doing so extend the sensed time range down to nanoseconds in a simple steady-state experiment. In the following sections we shall introduce experimental systems of MARY spectroscopy, outline its physical background, provide the relevant experimental details, and then apply it in its typical experimental setting.

1.1 Radical Ion Pairs in Nonpolar Solutions

The particular realization of MARY spectroscopy developed in this laboratory has as its objects of study spin-correlated radical ion pairs, generated by irradiating liquid alkane solutions of suitable charge acceptors in millimolar concentrations with an X-ray tube. Other possibilities that have been realized elsewhere include photoionization in nonpolar solutions [5] and photoinduced electron transfer in moderately polar solutions [6, 7]. The flux of X-ray quanta hitting the solution leads to ionization of the more abundant solvent molecule, knocking the electron as much as about 10 nm from its parent molecule and producing the primary radical ion pair of the solvent radical cation and the thermalized electron. The separation of the pair partners is well below the Onsager radius in the used solvent (about 30 nm for $\epsilon = 2$), so that the two charges are drawn to each other by Coulombic attraction and will eventually recombine.

Due to rather high electron mobility in nonpolar liquids the primary pair recombines within several picoseconds, which is too short to affect it by applying magnetic fields of convenient strengths. However, when a suitable electron acceptor is introduced in the solution, a radical anion with normal molecular mobility is formed, extending the lifetime of the pair into a more acceptable time range of several nanoseconds to tens of nanoseconds. Often the primary solvent radical cation is also captured by a suitable electron donor (i.e., hole acceptor). The acceptors are chosen by their ionization potential (IP for hole acceptor molecule should be lower than for solvent molecule to accept hole) and electron affinity (EA in solution for electron acceptor molecule should be positive to accept electron), and this choice is often flexible and nonrestricting enough to tailor the forming secondary radical ion pair to our needs. The pair will recombine in about 10 ns, depositing the energy stored in the electrostatic interaction into the energy of electronic excitation of one of the partner molecules.

The processes of ionization, charge transfer and recombination to good approximation do not affect spins of the involved radicals. Upon ionization the pair is normally created in spin-correlated singlet state, since the parent molecule had closed electronic shell. Upon recombination the multiplicity of the forming excited molecule is also the same as the multiplicity of the pair at the moment of recombination. And the spin state of the pair can change during the time interval from ionization to recombination, since the spins would couple to magnetic fields, internal or external. It takes about 10 G to alter the spin state of the pair in the

available 10 ns, and so this can be done controllably and predictably by applying a weak static external magnetic field or taking advantage of the internal hyperfine couplings in the radical ions of the pair. Recombination will then produce a singlet or triplet electronically excited molecule, and if the latter is a fair enough luminophore, singlet state can be detected by the quantum of fluorescence it emits, and triplet excited molecule in these conditions will deactivate radiationlessly.

Thus, recombination of the pair followed by optical detection with a photomultiplier tube (PMT) projects the pair onto its singlet state, and the signal from the PMT gives a direct measure of the fraction of pairs recombining in the singlet state, provided that they start also from singlet state. It is crucial here that recombination of the pair is not spin sensitive per se, but products of only one type (singlet) lead to observed signal. Magnetic interactions in the pair just switch the channels of reaction of recombination (into singlet or into triplet state). A further important simplification for radiation-generated radical ion pairs is that since the separation between the two radicals is fairly large all the time, spin-spin interactions (dipole-dipole and exchange) are so weak that they can be neglected. So conceptually we have a pair of two correlated but otherwise independent electron spins, starting from singlet state and producing the observed signal when recombining back into singlet state. The molecule motion is completely decoupled from spin evolution and just determines the lifetime distribution for the pairs. Of course the real situation is more complicated, but the provided picture grasps all the key features of our model objects.

1.2 Physical Background of MARY Spectroscopy

As was stated above, MARY spectroscopy relies on the coherent nature of the pair to derive its spectra, so we shall now briefly outline what goes on in the spin system of the pair. For our purpose the Hamiltonian of the pair can be written in the following form:

$$\mathcal{H} = g\beta\mathbf{H}(\mathbf{S}_1 + \mathbf{S}_2) + \sum a_i \mathbf{I}_i \cdot \mathbf{S}_1 + \sum a_j \mathbf{I}_j \cdot \mathbf{S}_2. \quad (1)$$

It includes only isotropic electron Zeeman and hyperfine interactions. Electron dipole-dipole and exchange interactions were omitted for reasons described above, all anisotropic contributions were neglected since in experiments non-viscous liquid solutions are used, and g -values for the two radicals were taken to be equal since only the region of weak magnetic field will be discussed in what follows. To calculate the experimental MARY spectrum $G(H)$, the time-dependent probability of finding the spin system in singlet state $\rho_{ss}(t, H)$ should be found by solving the Hamiltonian (1) and then convoluted with the recombination function $f(t)$

$$G(H) = \int \rho_{ss}(t, H) f(t) dt. \quad (2)$$

Due to hyperfine interactions of the two unpaired electrons with their nuclei, the initial singlet state of the pair is not its eigenstate, so we develop it into several eigenstates $|i\rangle$ that will then evolve with their own, generally different frequencies ω_i (see Fig. 1). To account for recombination into singlet state, the time-dependent state of the pair is projected back onto its singlet state, and interference terms of the form $B \cos(\Delta\omega_{ij}t)$ appear in $\rho_{SS}(t, H)$. If a time-resolved experiment is performed, these terms would produce the well-known quantum beats in recombination fluorescence [8]. However, in a stationary experiment such as MARY, $\rho_{SS}(t, H)$ is averaged over lifetime distribution $f(t)$ Eq. (2), and the oscillating terms vanish except for the fields when $\Delta\omega_{ij} \approx 0$, i.e., two or more eigenlevels cross. Since ω_i are the eigenvalues of the Hamiltonian (1) containing magnetic field H , they depend on H , and thus by sweeping H the condition of level crossing can be met. In ref. 9 it was shown that at these points the magnetic field dependence of the light coming from the sample will show sharp resonancelike lines (Fig. 2). The shape and width of the lines depend on the slopes of the intersecting eigenlevels of the Hamiltonian and on the recombination function $f(t)$, and for the exponential recombination kinetics the familiar Lorentzian contour emerges.

To observe the resonancelike lines, two conditions must be fulfilled: several eigenstates must be populated simultaneously from the initial singlet state of the pair, with some of them crossing at a certain field, and the time available for coherent spin evolution must be sufficient for several periods of internal spin motion so that the interference effects can fully develop. The latter condition can be quantified as [10]

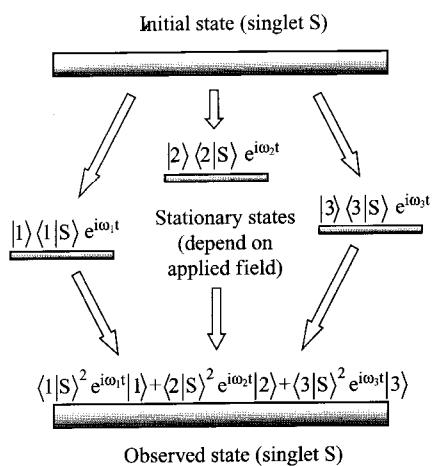


Fig. 1. Development of the interference effects in spin system of the radical pair that lead to MARY spectra. Several eigenstates of the pair's Hamiltonian are occupied from nonstationary initial state (singlet), which leads to time-dependent singlet contribution to the total wave function of the pair of spins, and thus to interference terms in $\rho_{SS}(t)$.

$$\Omega\tau^* \gg 1, \quad \Omega = \sqrt{\frac{1}{3} \sum a_i^2 I_i(I_i + 1)}, \quad \frac{1}{\tau^*} = \sum \frac{1}{\tau_a}. \quad (3)$$

Here Ω is the second moment of the ESR spectrum of the radical, which gives a measure of internal hyperfine fields in which the spin precesses in weak or zero external magnetic field, and τ^* is the lifetime of the coherent state of the pair, which is determined by several processes such as relaxation or chemical decay, which are exponential and are represented by their characteristic times τ_a . Furthermore, it was found advantageous if the dominant hyperfine couplings are concentrated in one of the pair partners, since this simplifies energy level layout of the system and makes the crossings more efficient. Experimental systems are usually chosen in such a way that one partner has substantial hyperfine couplings, i.e., large Ω – this is the “driver” of spin evolution in the pair that determines time sensitivity of the experiment –, while the other partner has negligibly small couplings, just complementing the pair. Ω in Eq. (3) refers to the driver.

Thus, if a suitable sample is put under stationary X-irradiation, its steady state fluorescence is monitored with a PMT, and external static magnetic field is applied and swept, from zero, the field dependence of fluorescence intensity will show a smooth rise due to gradual switching off of the T_{\pm} states of the pair by Zeeman interactions, onto which sharp resonancelike lines due to coherent evolution of the pair arise. The idea of studying field dependence of fluorescence, generally referred to as the magnetic field effect (MFE), has been actively exploited since 1970s and provided a large body of data on hyperfine couplings in short-lived radicals and radical ions [11]. However, it is the lines which will

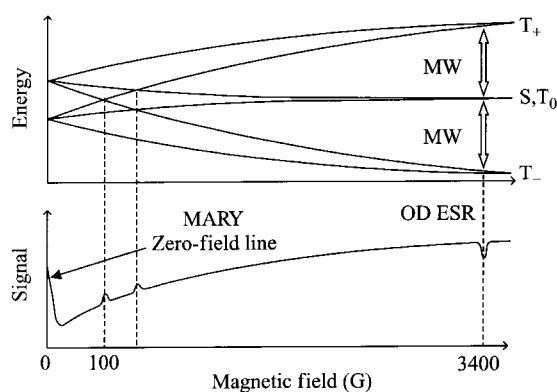


Fig. 2. Schematic energy level layout of spin system of the pair showing the crossings of the eigenlevels (top), and a sketch of the magnetic field dependence of the observed signal that it would produce. It is shown that at high field the eigenlevels converge into the singlet and triplet states of the pair, and if microwave pumping is applied to the system, an optically detected ESR signal can be observed at normal ESR field strengths. However, at the fields of the order of the hyperfine couplings in the partners of the pair (10–100 G), resonancelike MARY lines are observed without microwave pumping.

further be referred to as MARY lines that turn MFE into MARY spectroscopy, since their positions reflect the structure of the radicals, while their shape and width provide kinetic information. The lines arise in the fields of the order of the hyperfine coupling constants as well as at zero field. While MARY lines in nonzero fields have by now been reported only for systems with equivalent nuclei which have a particularly simple energy level layout [12, 13], the zero-field line is ubiquitous [10] and thus far more important. Qualitatively its origin is higher, spherical, symmetry of a system in zero magnetic field as opposed to lower, cylindrical, symmetry of a system in applied external field [14]. From now on only the zero-field line will be discussed.

1.3 Comparison with CW ESR

Let us compare MARY spectroscopy with its closest counterpart in conventional magnetoresonance techniques, CW ESR. MARY spectra are observed when the inequality Eq. (3) holds true, that is, coherent lifetime of the pair must allow for several periods of internal spin motion. To observe CW ESR spectra from short-lived radicals, microwave field H_1 in the resonator must be strong enough, $H_1\tau \gg 1$, to allow for several periods of spin precession about H_1 in the rotating frame during the lifetime of the pair τ . Regarding the attainable values of H_1 and Ω , we have H_1 typically not exceeding 1 G (for about 1 W of microwave power), while Ω , the second moment of the ESR spectrum of the driver partner of the pair, can be substantially higher, e.g., $\Omega(\text{C}_6\text{F}_6^-) = 230$ G. This in turn means that species with lifetimes two orders of magnitude shorter can be sensed by MARY as compared to ESR. Recalling the order of magnitude correspondence 1 G \leftrightarrow 100 ns, the practical limit for CW ESR (in any form) are lifetimes longer than about 100 ns, and as short as units of nanoseconds for MARY. The price for the extended time range is the lack of specificity: only a single line in zero field reflecting the processes in the spin system, on the background of MFE, is usually observed in MARY, while the entire spectrum can be obtained by ESR in favorable conditions.

2 Experimental Procedures

2.1 Experimental Setup

The scheme of the MARY spectroscopy setup currently in use in the authors' laboratory is shown in Fig. 3. About 1 ml of degassed solution is put in a quartz cuvette with a teflon stopcock. The cuvette is placed in the resonator of the commercial Bruker 200D CW ESR spectrometer equipped with an X-ray tube (BSV-27 Mo, 40 kV \times 20 mA) for sample irradiation and a PMT (FEU-130) with lightguide for fluorescence detection. No microwave power is applied to the sample. The ESR console provides only a single-polarity field sweep, so addi-

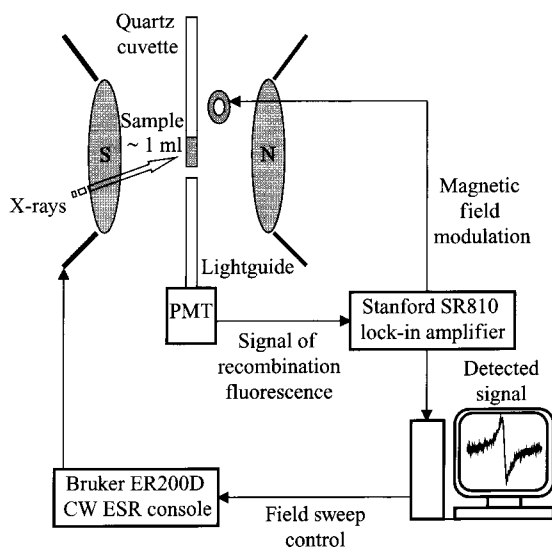


Fig. 3. Experimental setup of MARY spectroscopy (see text for explanation).

tional coils with a dedicated constant current source are put on the poles of the magnet to provide “negative” field shift. Since MARY lines are rather weak, field modulation and lock-in detection (Stanford SR-810 lock-in amplifier) of the fluorescence signal with computer averaging is used. In a typical experiment the field is swept from “−50” to “+50” G through zero with modulation amplitude 1–20 G at 12.5 kHz, lock-in detector is set to 1–3 s time constant and filter slope 6 dB/octave, 20 scans of 512 points with sweep rate 200–500 s per scan are taken and averaged in the controlling PC. Each spectrum takes 1–2 h to record.

2.2 General Look of MARY Spectra

A general view of a MARY spectrum is shown in Fig. 4. Because of field modulation, the spectrum is first derivative and it is symmetric about the zero of the field. The reference features of the spectrum are the wings of the MFE, with characteristic inflection point $B_{1/2}$, and the “inverted” zero-field MARY line with characteristic peak-to-peak width ΔH_{pp} . Although generally a complete simulation of the spectrum is required to get numerical results, the following useful estimates (strictly valid in the conditions of isolated MARY line) can be obtained

$$B_{1/2} = 2 \frac{\Omega_1^2 + \Omega_2^2}{\Omega_1 + \Omega_2}, \quad \Delta H_{pp} (G) = \frac{66}{\tau^* (\text{ns})}, \quad (4)$$

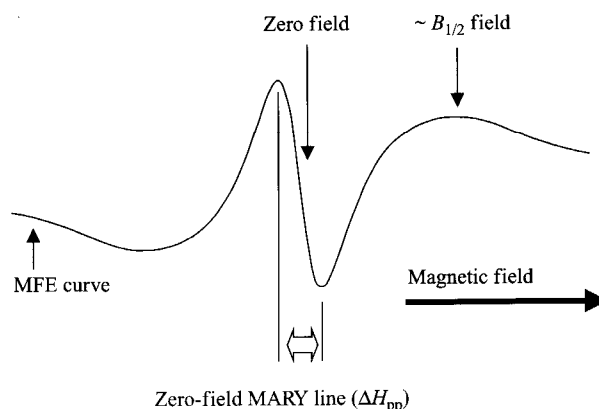


Fig. 4. Typical view of the MARY spectrum in the vicinity of zero field (see text for explanation).

where $\Omega_{1,2}$ are second moments of the ESR spectra of the pair partners, and τ^* is the coherent lifetime of the pair. The $B_{1/2}$ estimate becomes especially valuable when the dominant hyperfine couplings are condensed in one of the pair partners, say, $\Omega_1 \gg \Omega_2$. $B_{1/2}$ then gives a direct measure of the gross hyperfine couplings in the driver radical ion, and is very helpful in identifying the partners of the recombining pair. The zero-field line is a direct reporter of fast processes that the partners of the pair are involved in, including internal spin relaxation, chemical decay, and the reaction of degenerate electron exchange between the radical ion and its neutral parent molecule, further referred to as the DEE reaction.

3 Typical Applications of MARY Spectroscopy

The effect of level crossing for radical ion pairs is very interesting in itself. Similar effects have long been known and used in atomic spectroscopy (Hanle effect in atomic fluorescence, 1924 [15]), molecular spectroscopy (level crossing and anticrossing spectroscopy of simple molecules based on Stark effect, 1960s, e.g., [16]), solid-state physics (level crossing spectroscopy of semiconductor superlattices, 1990s, e.g., [17]), only in MARY spectroscopy we deal not with rarefied sodium vapors and regular crystal structures at 4 K, but with warm liquids and radical ions having lifetimes as short as nanoseconds. And as with other effects, level crossing gains practical significance when it goes beyond being mere technique for technique's sake and is applied to solve real problems. We shall now briefly describe two of them, which will expose the approaches for application of MARY spectroscopy at its current level of development that take full advantage of its exceptional time sensitivity for a stationary spin-sensitive technique, while alleviating its limitations of the poor specificity.

3.1 Radical Cation of *trans*-Decalin

The first example is the problem of radical cation of *trans*-decalin [18]. Decalin, or decahydronaphthalene, can exist as two stable stereoisomers, *cis*- and *trans*-decalin. While radical cation of *cis*-decalin behaves normally for an alkane radical cation and yields good optically detected (OD) ESR spectra even at room temperature, its *trans* counterpart shows no spectra at temperatures above 150 K. However, rather good MARY spectra were obtained at room temperature, from which it was deduced that radical cation of *trans*-decalin has very short relaxation time of only 7 ns (in low magnetic field). This provided a clue from which the complete temperature dependence of the OD ESR spectra was successfully described. The reason for such a short relaxation time was found to be the near degeneracy of the electronic state of the radical cation and its ensuing Jahn–Teller activity.

3.2 Short-Lived Biradical Ions

Another example is a recent study of short-lived biradical ions in spin triads of the type “radical ion–biradical ion” [19]. This problem emerged from the interest in the phenomenon of spin catalysis – the effect of the “external” spin on coherent evolution of a spin system [20]. To this end, several spin-labeled charge acceptors with the structure “stable 2-imidazoline radical–hydrocarbon bridge–aromatic charge acceptor” were synthesized. Under irradiation in nonpolar solution they yield biradical ions with the spins of the stable radical and the radical ion moiety coupled through the bridge. As always, the pair is complemented with the other radical ion of the opposite charge so that a spin-correlated radical ion pair is produced in which one of the pair partners is magnetically coupled to the “external” spin of the stable radical moiety of the spin-labeled acceptor. However, the spin chemistry experiments with these systems (time-resolved magnetic field effects and OD ESR) proved to be very laborious and not too successful, with the probable reason being too strong a coupling in the biradical ion. MARY spectroscopy was then used for a systematic structure scan of about 20 target substances to reduce the coupling until the signal appeared. After that, the best system found was studied with CW ESR and OD ESR, and an estimate of $J \approx 10^3$ G was obtained. Here again MARY spectroscopy provided the needed clue for application of the more specific, but also much more demanding magnetoresonance techniques.

3.3 Typical Approaches of MARY Spectroscopy

Let us now briefly summarize the practical aspects and the possible approaches of the MARY spectroscopy technique. The best system for MARY is a warm nonpolar solution being a difficult system for most other spin-sensitive techniques.

A good fluorescing electron donor or acceptor is required, but in exchange only spin-correlated radical ion pairs containing the luminophore contribute to the observed signal, ruling out numerous background processes that plagued traditional radiation chemistry studies. The method can sense coherent lifetimes of the system down to nanoseconds. In fact, longer characteristic times are not always preferable, as the region of maximum sensitivity is determined by hyperfine couplings in the driver partner of the pair. The technique has a preferred window at the time scale, which can be adjusted in the region from units to hundreds of nanoseconds by choosing an appropriate driver. The technique senses gross hyperfine structure (second moment of the ESR spectrum) via the wings of the MFE curve, and dynamic processes that affect coherent spin evolution (via the shape and width of the zero-field MARY line). However, "sense" is the key word here, since the technique lacks spectral specificity and discrimination. As of today, useful practical applications of MARY spectroscopy would mostly include getting clues for more elaborate and demanding spin chemistry techniques like OD ESR and time-resolved studies, or application to a series of similar compounds that can be directly compared. We shall adopt the latter approach for the study of radical cations of methyl-substituted benzenes described in the following sections.

4 Radical Cations of Methyl-Substituted Benzenes

The interest towards short-lived radical cations of methyl-substituted benzenes is connected with another facet of MARY spectroscopy – its biological implications. The presence of the sharp line at zero magnetic field implies that rather weak static magnetic fields can alter the course of chemical and biochemical reactions having radical pairs as intermediates. The narrowest line seen to date in this laboratory had peak-to-peak width of only 2.5 G (durene plus *p*-terphenyl- d_{14} in squalane), and in theory the line can be still narrower, provided the coherent lifetime of the pair is long enough [21]. This already comes close to the geomagnetic field strengths (about 0.5 G), and can probably provide a mechanism for biological action of geomagnetic fields [22, 23].

One of the possibilities to controllably alter coherent lifetime of the pair is to introduce fast paramagnetic relaxation in one of the pair partners. Bearing this in mind, we took a series of eight methyl-substituted benzenes from benzene to hexamethylbenzene (HMB) shown in Fig. 5, which are all good hole acceptors in alkane solution. Figure 5 also shows hyperfine couplings for radical cations of the benzenes (when they are known) and calculated second moments of their ESR spectra. No data was found on radical cation of *o*-xylene, but possibly this is because it was not studied earlier. More important are the two leftmost species, benzene and mesitylene (*sym*-trimethylbenzene). Although the couplings for benzene radical cation are known and shown in Fig. 5, no OD ESR spectra have ever been reported for it in liquid alkane solution despite substantial effort put into such studies. Regarding mesitylene, no positive results on its radical cation have been found in literature at all, although OD ESR studies were also attempted

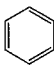
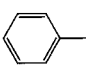
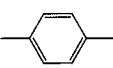
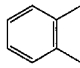
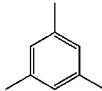
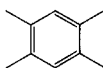
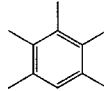
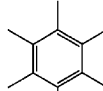
			
Benzene 6H: 3.75 $\Omega = 6.5$	Toluene 3H(CH ₃): 20.0 4H: 12.5 $\Omega = 30.2$	para-Xylene 6H(CH ₃): 18.3 4H: 3.0 $\Omega = 32.0$	ortho-Xylene ???
			
Mesitylene ???	Durene 12H(CH ₃): 11.5 $\Omega = 28.2$	Pentamethyl- benzene 12H(CH ₃): 10.1 3H(CH ₃): 0.3 H: 0.3 $\Omega = 24.6$	Hexamethyl- benzene 18H: 6.5 $\Omega = 19.3$

Fig. 5. Structural formulae, hyperfine coupling constants, and second moments of ESR spectra of radical cations (Ω) for benzene and seven methyl-substituted benzenes studied in this work.

[24]. The reason called upon to explain the lack of OD ESR spectra was presumably fast internal paramagnetic relaxation of the two radical cations due to their high symmetry and probable Jahn–Teller activity. Indeed, of the eight molecules only three formally have threefold or higher symmetry: benzene and HMB (D_{6h}) and mesitylene (D_{3h}), but HMB is probably nonplanar due to six methyls. The other 5 molecules have either C_{2v} or D_{2h} point groups and thus no forced electronic degeneracy. Point groups of benzene and mesitylene molecules have doubly degenerate irreducible representations and twofold electronic degeneracy of the semioccupied orbital in radical cation. Thus, we have a series of similar species, with similar hyperfine couplings, but presumably very fast relaxation in two of them. We shall now apply MARY spectroscopy to check this.

4.1 Identifying Radical Cations by Their MARY Spectra

Figure 6 shows a selection of MARY spectra from a typical concentration dependence, in this case for durene in cyclohexane. 10^{-4} M *p*-terphenyl- d_{14} (PTP) was added to solution as electron acceptor and luminophore. Cyclohexane was chosen because of the exceptionally high mobility of its radical cation (solvent hole), which is about 30 times higher than molecular mobility in this solvent [25]. This allows one to use lower concentrations of hole acceptors, which reduces the rate of the DEE reaction that contributes to spin relaxation completely similar to CW ESR. As can be seen, no spectra are observed at the lowest displayed concentration of durene, since the concentration C (10^{-4} M) is too low to produce durene radical cations in substantial amounts: for the rate of hole scavenging K of about 30 times 10^{10} ($3 \cdot 10^{11} \text{ M}^{-1}\text{s}^{-1}$) the characteristic scavenging

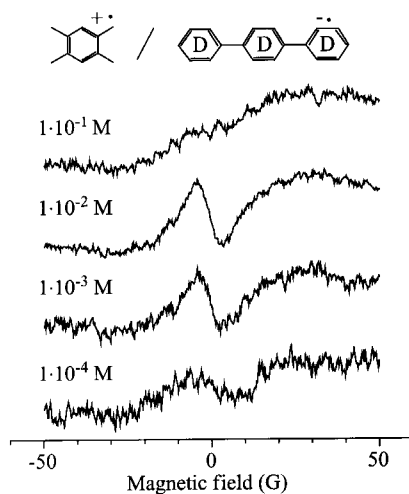


Fig. 6. Experimental MARY spectra of durene solutions in cyclohexane, room temperature. Durene concentration is shown to the left of each spectrum. 10^{-4} M PTP was introduced into solutions as electron acceptor and luminophore.

time $\tau \sim (KC)^{-1} \sim 30$ ns, which should be compared with typical recombination times of about 10 ns. As the concentration of durene is increased, a MARY spectrum arises with zero-field line and MFE wings. As the concentration is further increased up to 0.1 M, the line completely disappears, as the coherence in the pair is destroyed by the DEE reaction: characteristic residence time for the hole on a durene molecule $\tau \sim (10^{-1} \cdot 10^{10})^{-1} \sim 1$ ns. The inflection point of the MFE curve is consistent with Ω for durene (see simulations below), and the concentrational variation of the shape of MARY line is consistent with changes in concentration of durene. This set of spectra is sufficient to unequivocally ascribe the observed signal to the durene⁺-PTP⁻ pair and obtain the rate constant of the DEE reaction [26], which turns out to be diffusion-controlled here. For convenience we shall further refer to such spectra as simply “MARY spectra of durene”. We also pick the optimal concentration (10^{-2} M) for further discussion. The described experimental procedure was performed for all of the eight target substances, and all of them yielded consistent MARY spectra (with peculiarities for benzene; see below).

Figure 7 shows MARY spectra for the eight substances at the concentration of 10^{-2} M, and it can be noted that six of the spectra are very similar, while the top two, for benzene and for mesitylene, stand apart from the others: there is no MARY line for benzene, and only a rather weak one for mesitylene. We now recall that MARY line reports coherent lifetime of the pair, and that these two species were the candidates for the shorter relaxation time, and thus shorter coherent lifetime. Is this the sought clue? To answer this question, we take a closer inspection of the two candidates.

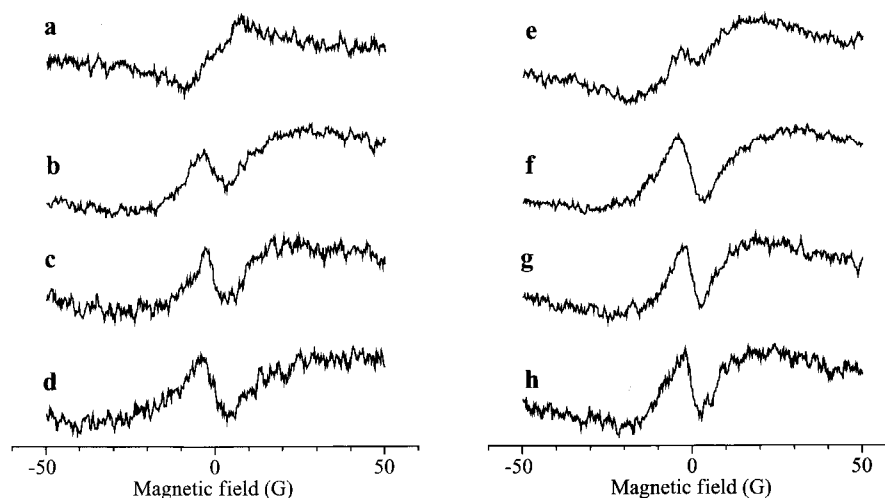


Fig. 7. Experimental MARY spectra for solutions of 10^{-2} M benzenes and 10^{-4} M PTP in cyclohexane, room temperature: benzene (a), toluene (b), *o*-xylene (c), *p*-xylene (d), mesitylene (e), durene (f), pentamethylbenzene (g), hexamethylbenzene (h).

4.2 Case Study of Benzene

In the case of benzene radical cation, when there is no MARY line at all, it is first necessary to verify ascription of the spectra, since concentrational studies in this case are not conclusive. To do this, we compare MARY spectra of benzene and deuterated benzene (Fig. 8, left). It is seen that deuteration reduces the width of the MFE, as it should since complete deuteration reduces the second moment of the ESR spectrum of the radical 4 times as compared to the proton-containing counterpart. The second moment of PTP $^{\cdot-}$, 0.7 G, is small enough for the inequality $\Omega_1 \gg \Omega_2$ to hold, so the positions of the inflection points at the wings of the spectra give direct measure of hyperfine couplings in the radical cation. Simple calculation gives peak-to-peak values $\Delta B_{1/2H} \sim 25$ G, $\Delta B_{1/2D} \sim 6$ G, in good agreement with experiment.

This idea of deuteration can also be exploited to demonstrate that the absence of MARY line for benzene is explained by its smaller hyperfine couplings as compared to methyl-substituted benzenes. Figure 8 shows MARY spectra of benzene, toluene, and their deuterated analogues. Toluene, having $\Omega = 30.2$ G, shows a pronounced MARY line in the zero field, which completely disappears upon deuteration. Deuteration in this case reduces Ω of the radical cation from 30.2 down to 7.5 G, which is close to 6.5 G of the benzene radical cation, and the spectrum of toluene is nearly transformed into the spectrum of benzene. Qualitatively weaker hyperfine couplings in the radical cation mean a weaker driver of spin evolution in the pair: the 6.5 G of benzene radical cation translate into the characteristic time of internal spin motion of 10 ns, which is just the characteristic

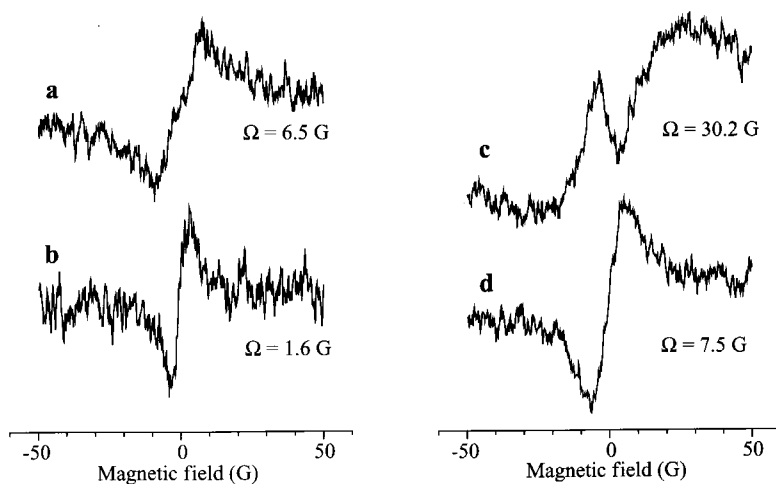


Fig. 8. Experimental MARY spectra for solutions of 10^{-2} M benzenes and 10^{-4} M PTP in cyclohexane, room temperature: benzene (a), benzene- d_6 (b), toluene (c), toluene- d_8 (d). Also shown are second moments of ESR spectra of the radical cations.

recombination time for this system, and the interference effects do not develop. The spectrum of benzene is too poor in features to be modeled, and this qualitative conclusion is deemed sufficient here.

4.3 Case Study of Mesithylene

Let us now turn to mesithylene and compare it with durene. Figure 9 shows MARY spectra of durene and mesithylene (left), and the results of simple simulation in the exponential model of recombination and semiclassical model of spin motion [27]. Second moments of ESR spectra of the partners in modeling were taken to be 28 G (durene, the driver) and 0 G (PTP, complementing the pair), recombination time $\tau_0 = 10$ ns for all curves. Furthermore, additional exponential relaxation with characteristic times $\tau = 8, 6, 4, 2$ ns (top to bottom) was introduced in simulations. The bold lines show the closest matches to experimental spectra for durene ($\tau = 6$ ns) and mesithylene ($\tau = 2$ ns). As can be seen, shorter relaxation times indeed dampen the MARY line. The model spectra are somewhat rounder than the experimental traces, which is a consequence of using simple exponential recombination function in modeling. An account for the nonexponentiality of recombination kinetics indeed sharpens the spectra and makes quantitative correspondence with experiment better [28], but significantly complicates the modeling without bringing further qualitative insights, so we shall refrain from it here.

The 6 ns of relaxation time for durene corresponds to the diffusion-controlled DEE reaction with the rate constant $K = (1-2) \cdot 10^{10} \text{ M}^{-1}\text{s}^{-1}$ at the used con-

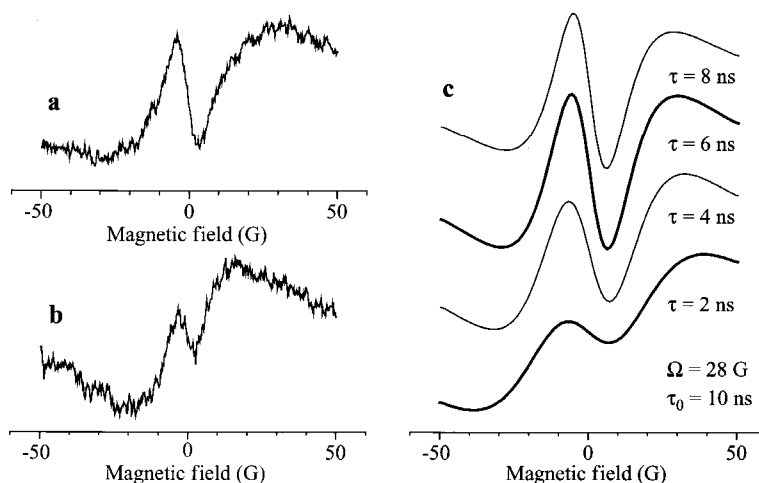


Fig. 9. Experimental MARY spectra for solutions of 10^{-2} M durene (a) or 10^{-2} M mesitylene (b) and 10^{-4} M PTP in cyclohexane, room temperature. c Simulation of the spectra in the model of exponential recombination kinetics with characteristic recombination time $\tau_0 = 10$ ns and semiclassical model of spin motion in the radical cation with second moment of ESR spectrum $\Omega = 28$ G (durene). Additional exponential relaxation with characteristic times $\tau = 8, 6, 4, 2$ ns introduced into simulations.

centration of durene 10^{-2} M, and thus reflects the unavoidable reaction of the radical cation rather than its internal relaxation. However, the exchange contribution in the mesitylene spectrum should be the same, since in the conditions of this experiment both systems are in the regime of slow exchange, and, as in CW ESR, the rate of induced relaxation is given just by the inverse of the characteristic residence time $\tau_{\text{res}} = [KC]^{-1}$ and does not depend on the system. So does the implied shorter relaxation time of 2 ns for mesitylene mean fast internal relaxation with characteristic time of several nanoseconds?

The answer to this question is “not necessarily”. A closer inspection of the spectra for durene and mesitylene (Fig. 9) shows that the width of MFE for the two systems is different, which means that hyperfine couplings in the two radical cations are different. Nothing was found in literature on the couplings in the mesitylene radical cation, but from Fig. 9 it can be inferred that the second moment of its ESR spectrum Ω is with experimental accuracy half Ω for durene radical cation, that is about 14 G. So, as in the case of benzene, we again return to the situation of a weaker driver of spin evolution. Figuratively speaking, radical pair does not measure magnetic field in Gauss and time in nanoseconds, it rather measures the field in units of Ω and time in units of the period of internal spin motion, which is inversely proportional to Ω . A reduction in Ω means expansion of the reduced field scale and contraction of the reduced time scale for the pair relative to given absolute field and time scales.

A vivid illustration of this is given in Fig. 10, which again shows MARY spectra for durene and mesitylene and their simulation. The model spectra were

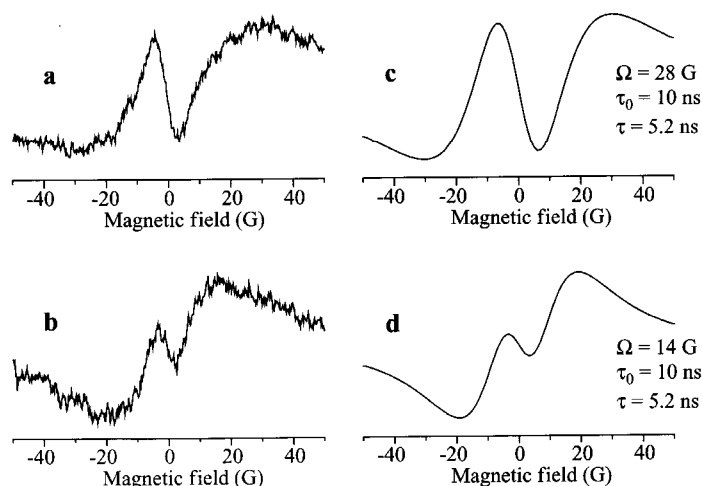


Fig. 10. Experimental MARY spectra for solutions of 10^{-2} M durene (a) or 10^{-2} M mesitylene (b) and 10^{-4} M PTP in cyclohexane, room temperature; simulation of the spectra with $\tau_0 = 10$ ns, $\tau = 5.2$ ns, and $\Omega = 28$ G (c, durene) and 14 G (d, mesitylene).

obtained in the following manner: first the spectrum for durene was simulated using the known value of its Ω (28 G), setting recombination time to 10 ns, and varying relaxation time to obtain the best fit in this model, which produced the value of 5.2 ns and the spectrum shown in Fig. 10c. Then Ω was reduced from 28 to 14 G, and a spectrum with the same times was calculated. It is shown in Fig. 10d and reproduces the experimental MARY spectrum for mesitylene quite well. Thus we can conclude that no relaxation processes with characteristic times of several nanoseconds or shorter (the time window of the current experiment) are present in the radical cation of mesitylene.

5 Conclusion and Outlook

This completes the exposition of the practical aspects of the technique of MARY spectroscopy as developed in the authors' laboratory. We have discussed the underlying principles of the technique, addressed its key practical advantages and limitations, and demonstrated a typical pattern of thinking in performing MARY studies. Further development of the technique, both in methodology and in practical applications, is currently on its way. As a practical outcome we have demonstrated that radical cations of benzene and mesitylene have relaxation times not shorter than about several nanoseconds – the time scale of the current MARY experiment, which can be taken as a clue to undertake OD ESR studies for obtaining more specific spectral information. This is particularly important for radical cation of mesitylene, for which no data have been found in literature.

Acknowledgements

We are indebted to F. Sviridenko for helpful comments on this manuscript. The work was supported by RFBR, project 03-03-32331, and MinVuz, project E02-5.0-49. D.V.S. is grateful to the Russian Science Support Foundation for awarding a personal scholarship.

References

1. Salikhov K.M., Molin Yu.N., Sagdeev R.Z., Buchachenko A.L.: Spin Polarisation and Magnetic Effects in Radical Reactions. Amsterdam: Elsevier 1984.
2. Nagakura S., Hayashi H., Azumi T. (eds.): Dynamic Spin Chemistry. Tokyo, New York: Kodansha, Wiley 1998.
3. Salikhov K.M., Sakaguchi Y., Hayashi H.: Chem. Phys. **220**, 355–371 (1997)
4. Tadjikov B.M., Astashkin A.V., Sakaguchi Y.: Chem. Phys. Lett. **284**, 214–220 (1998)
5. Saik V.O., Ostafin A.E., Lipsky S.: J. Chem. Phys. **103**, 7347–7358 (1995)
6. Hamilton C.A., Hewitt L.J.P., McLauchlan K.A., Steiner U.E.: Mol. Phys. **65**, 423–438 (1988)
7. Grampp G., Justinek M., Landgraf S.: Mol. Phys. **100**, 1063–1070 (2002)
8. Bagryansky V.A., Usov O.M., Borovkov V.I., Kobzeva T.V., Molin Yu.N.: Chem. Phys. **255**, 237–245 (2000)
9. Sukhenko S.A., Purtov P.A., Salikhov K.M.: Khim. Fiz. **1**, 21–27 (1983)
10. Stass D.V., Lukzen N.N., Tadjikov B.M., Molin Yu.N.: Chem. Phys. Lett. **233**, 444–450 (1995)
11. Steiner U.E., Ulrich T.: Chem. Rev. **89**, 51–147 (1989)
12. Stass D.V., Tadjikov B.M., Molin Yu.N.: Chem. Phys. Lett. **235**, 511–516 (1995)
13. Grigoryants V.M., McGrane S.D., Lipsky S.: J. Chem. Phys. **109**, 7354–7361 (1998)
14. Salikhov K.M.: Chem. Phys. **82**, 145–162 (1983)
15. Moruzzi G., Strumia F. (eds.): The Hanle Effect and Level Crossing Spectroscopy. New York: Plenum 1991.
16. Zare R.N.: J. Chem. Phys. **45**, 4510–4518 (1966)
17. Mashkov I.V., Gourdon C., Lavallard P., Roditchev D.Yu.: Phys. Rev. **55**, 13761–13770 (1997)
18. Tadjikov B.M., Stass D.V., Molin Yu.N.: J. Phys. Chem. A **101**, 377–383 (1997)
19. Sviridenko F.B., Stass D.V., Kobzeva T.V., Tretiakov E.V., Klyatskaya S.V., Mshvidobadze E.V., Vasilevsky S.F., Molin Yu.N.: J. Am. Chem. Soc. **126**, 2807–2819 (2004)
20. Buchachenko A.L., Berdinsky V.L.: Chem. Rev. **102**, 603–612 (2002)
21. Timmel C.R., Till U., Brocklehurst B., McLauchlan K.A., Hore P.J.: Mol. Phys. **95**, 71–89 (1998)
22. Ritz T., Adem S., Schulten K.: Biophys. J. **78**, 707–718 (2000)
23. Brocklehurst B.: Chem. Soc. Rev. **31**, 301–311 (2002)
24. Saik V.O., Anisimov O.A., Lozovoy V.V., Molin Yu.N.: Z. Naturforsch. A **40**, 239–245 (1985)
25. Shkrob I.A., Sauer M.C. Jr., Trifunac A.D.: J. Phys. Chem. **100**, 7237–7245 (1996)
26. Stass D.V., Lukzen N.N., Tadjikov B.M., Grigoryantz V.M., Molin Yu.N.: Chem. Phys. Lett. **243**, 533–539 (1995)
27. Schulten K., Wolynes P.G.: J. Chem. Phys. **68**, 3292–3297 (1978)
28. Toropov Yu.V., Sviridenko F.B., Stass D.V., Doktorov A.B., Molin Yu.N.: Chem. Phys. **253**, 231–240 (2000)

Authors' address: Evgeny V. Kalneus, Institute of Chemical Kinetics and Combustion, Russian Academy of Sciences, Institutskaya ulitsa 3, Novosibirsk 630090, Russian Federation
E-mail: kalneus@ns.kinetics.ncs.ru